

Article

An Efficient 4H-SiC Photodiode for UV Sensing Applications

Mohamed L. Megherbi¹, Hichem Bencherif² , Lakhdar Dehimi¹, Elisa D. Mallema³, Sandro Rao^{3,*} , Fortunato Pezzimenti³ and Francesco G. Della Corte⁴ 

- ¹ LMSM—Laboratory of Metallic and Semiconducting Materials, University of Biskra, Biskra 07000, Algeria; mlmegherbi@yahoo.fr (M.L.M.); la_dehimi@yahoo.fr (L.D.)
- ² LAAAS—Laboratory, Mostefa Benboulaïd University, Batna 05000, Algeria; hichembencherifeln@gmail.com
- ³ Department DIIES, Mediterranean University, 89124 Reggio Calabria, Italy; elisa.mallema@unirc.it (E.D.M.); fortunato.pezzimenti@unirc.it (F.P.)
- ⁴ Department DIETI, University of Naples Federico II, 80125 Naples, Italy; francescogiuseppe.dellacorte@unina.it
- * Correspondence: sandro.rao@unirc.it

Abstract: In this paper, we report experimental findings on a 4H-SiC-based p-i-n photodiode. The fabricated device has a p-type region formed by ion-implantation of aluminum (Al) in a nitrogen doped n-type layer. The dark reverse current density reaches 38.6 nA/cm² at −10 V, while the photocurrent density rises to 6.36 μA/cm² at the same bias under λ = 315 nm ultraviolet (UV) radiation with an incident optical power density of 29.83 μW/cm². At the wavelength of λ = 285 nm, the responsivity is maximum, 0.168 A/W at 0 V, and 0.204 A/W at −30 V, leading to an external quantum efficiency of 72.7 and 88.3%, respectively. Moreover, the long-term stability of the photodiode performances has been examined after exposing the device under test to several cycles of thermal stress, from 150 up to 350 °C and vice versa. The achieved results prove that the examined high-efficiency UV photodiode also has a stable responsivity if subjected to high temperature variations. The proposed device is fully compatible with the conventional production process of 4H-SiC components.

Keywords: 4H-SiC; p-i-n photodiode; temperature effect; responsivity



Citation: Megherbi, M.L.; Bencherif, H.; Dehimi, L.; Mallema, E.D.; Rao, S.; Pezzimenti, F.; Della Corte, F.G. An Efficient 4H-SiC Photodiode for UV Sensing Applications. *Electronics* **2021**, *10*, 2517. <https://doi.org/10.3390/electronics10202517>

Academic Editors: Tae-Yeon Seong, Slawomir Sujecki, Dong-Seon Lee, Noel Rodriguez, Changhwan Shin and Geok Ing Ng

Received: 3 September 2021
Accepted: 12 October 2021
Published: 15 October 2021

Publisher's Note: MDPI stays neutral with regard to jurisdictional claims in published maps and institutional affiliations.



Copyright: © 2021 by the authors. Licensee MDPI, Basel, Switzerland. This article is an open access article distributed under the terms and conditions of the Creative Commons Attribution (CC BY) license (<https://creativecommons.org/licenses/by/4.0/>).

1. Introduction

Ultraviolet detectors have significant uses in different areas, from astronomy to combustion control in the automotive industries, etc. [1]. The cost and the volume of the commonly used UV photomultipliers are still high, and the sensitivity to thermal stress remains a critical issue [2]. For these reasons, compact and affordable semiconductors photodiodes are suitable alternatives [3].

Supported by its distinguished properties, such as high thermal conductivity, wide band gap and critical breakdown strength, Silicon Carbide (SiC) is an intriguing choice for UV detection applications, also when the exposure to high temperatures could be an issue [4–7]. SiC photodiodes respond to light from short to long UV waves (200–400 nm), with reduced noise due to visible or infrared radiation [8,9].

Although photodiodes made in 6H-SiC have been examined in earlier time studies [10], the 4H-SiC polytype has gained much more attention in different application fields in the meantime [11,12] thanks to its improved electronic properties [13,14]. 4H-SiC-based photodiodes, in particular Schottky [15,16] and avalanche devices [17–19], have been extensively demonstrated in the last few years; only a few examples are reported instead for p-i-n structures [20–22], although they are more efficient from the optical-electrical conversion point of view.

Hereafter, we report the characteristics of an experimental 4H-SiC p-i-n UV photodiode showing a higher responsivity peak with respect to similar devices that have appeared to date in the literature [15–22]. Moreover, the fabricated devices have been stressed by temperature in order to investigate the effects on the electro-optical characteristics after

a long exposure, in a thermostatic chamber, to cycling temperature ramps, up to 350 °C. Results show that, within this temperature range, the photodiode does not modify its output characteristics also after many days from the first characterization.

2. Experiments

The studied and experimentally characterized photodiode is an integral part of a microchip processed by the CNR-Institute for Microelectronics and Microsystem of Bologna (Italy) [23]. Figure 1 shows the device cross-section, together with the main geometric dimensions, of the silicon carbide p-i-n structure considered in this work.

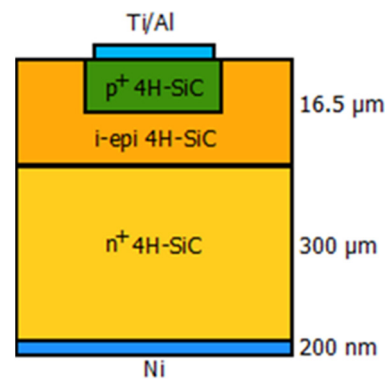


Figure 1. Schematic cross-section of a 4H-SiC photodiode.

The p-i-n diodes were manufactured on commercial, 300-micrometer-thick, n+ type 4H-SiC wafers [24], 100 mm in diameter, on which a homo-epitaxial layer with orientation $\langle 0001 \rangle$ and conductivity equal to $0.021 \Omega \cdot \text{cm}$ was grown. The region that forms the p-type anode, with a circular area of $9.62 \times 10^{-4} \text{ cm}^2$ (350 μm in diameter), was obtained by ionic implantation of aluminum (Al), while photolithographic processes and chemical etchings were used to create the upper concentric Ti/Al anode electrical contact, $2.41 \times 10^{-4} \text{ cm}^2$ (175 μm in diameter). Many p-i-n diodes were fabricated in the same microchip with the common cathode consisting of the n+ 4H-SiC substrate. More details about the manufacturing process are given in references [25,26]. To allow easy and stable electrical connections from the chip to the measurement set-up, each anode electrode was contacted by ultrasonic wire-bonding, using a thin Al-wire 50 μm in diameter. Finally, the chip was encapsulated in a custom package for optical and thermal characterization.

3. Results and Discussions

The characterization of the 4H-SiC photodiode was performed in a dark box at room temperature (RT) in order to obtain I–V characteristics in the absence of environmental interferences. Figure 2 reports the typical J–V characteristic of the investigated photodiode in forward bias, from 0 to 3 V. From this figure, it is evident that the current shows the set-up of an efficient carrier injection regime starting from a $\sim 1.5 \text{ V}$ anode bias.

Moreover, the series resistance, R_s , and the ideality factor, η , have been extracted from the forward J–V characteristics. By fitting the analytic diode equation, the values of R_s and η are extracted to be 489 Ω and 1.8, respectively, suggesting a good quality of p-i-n junction [21,27].

Figure 3 shows the J–V characteristic in reverse bias condition from 0 to -30 V . From this figure, an increasing reverse current density J_D is observed with voltage, reaching 22.3 and 78.6 nA/cm^2 , respectively at -5 and -30 V .

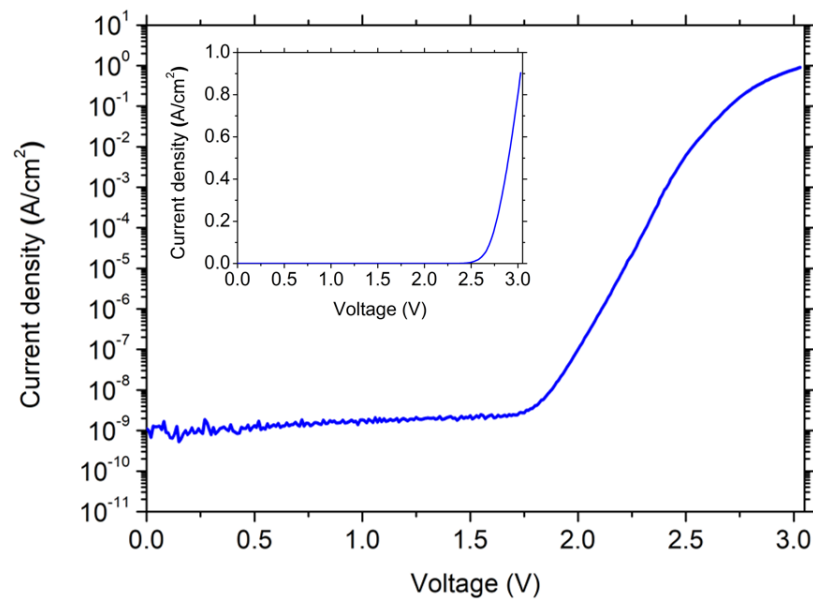


Figure 2. Current density vs. voltage characteristic at RT in forward bias from 0 to 3 V, in dark conditions. The insert reports the J–V characteristic in linear scale.

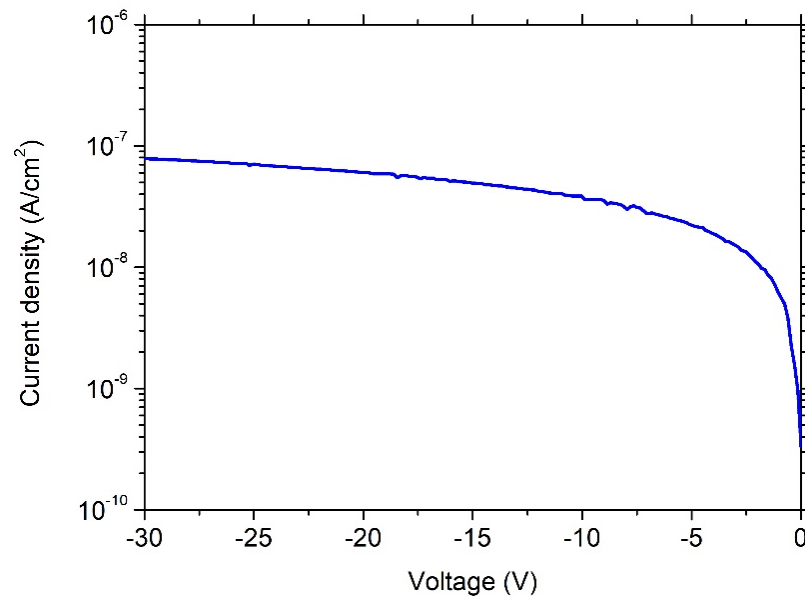


Figure 3. Current density–voltage characteristic, in dark conditions at RT, for reverse biases from 0 to –30 V.

By exposing the photodiode to a UV radiation produced by a remotely controlled monochromator, we measured the J–V characteristics at varying wavelengths, as shown in Figure 4 for specific wavelengths and incident optical powers. Electro-optical measurements were performed in the wavelength range between 210 and 380 nm, in steps of 5 nm. As the wavelength increases, we observe that the photocurrent increases, reaching its maximum value at 315 nm. At this wavelength, for which the optical power density at the surface is 29.83 nW/cm², the total current density is 5.44 μ A/cm² at 0 V, increasing to 6.88 μ A/cm² at –30 V. It should be noted that the photo-generated current amplitude is relevant with respect to the dark current, in spite of the low incident optical power at the surface.

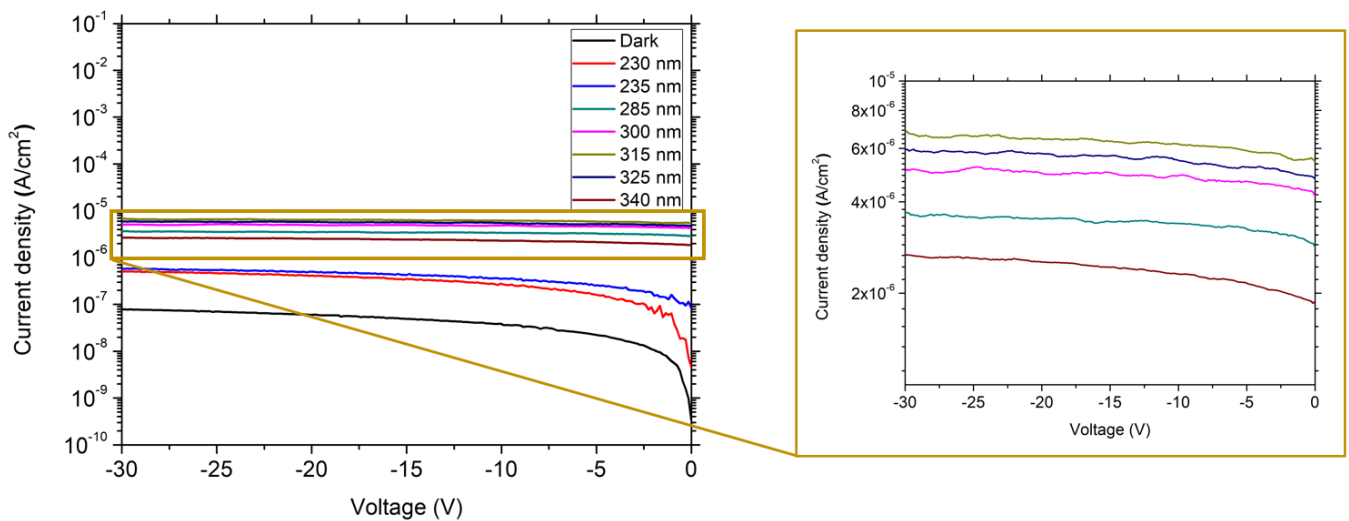


Figure 4. J–V characteristics for different UV wavelengths at RT. The incident optical power, from a monochromator, varies with the wavelength.

Figure 5 plots the photocurrent density as a function of the wavelength at 0 and 30 V reverse-biased values.

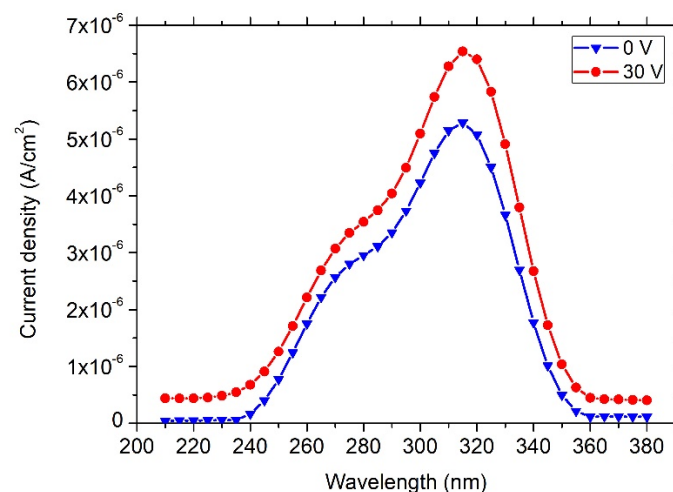


Figure 5. Photocurrent density as a function of the wavelength values at 0 and 30 V reverse bias.

The photocurrent shows a peak at a 315-nanometer wavelength; however, this depends on the wavelength-dependent incident optical power. For this reason, a full characterization of the monochromator was performed in order to calculate the optical power spectrum at a distance, from the UV radiation generator output surface, of 7 cm. A commercial DET 210 photodiode [28], with known active area and fully characterized responsivity, $R(\lambda)$ at all wavelengths, was used. The measured output voltage signal (V) is proportional to the direct photocurrent at the photodiode anode, function of the incident light power (P) and wavelength according to the following:

$$P = \frac{V}{R(\lambda)R_{\text{load}}} \quad (1)$$

where R_{Load} is an external load resistance of 50 ohm.

From the calculation of the active area of the 4H-SiC photodiode shown in Figure 1, a circular crown of area $7.21 \times 10^{-4} \text{ cm}^2$, and the corresponding incident optical power at each wavelength, the responsivity of the 4H-SiC photodiode under the UV radiation from the monochromator has been extracted. The responsivity, that is a figure of merit for

detection, measures the ratio of the photogenerated current (I_{ph}) to the incident optical power (P), and can be calculated from the following relation:

$$R = \frac{I_{ph}}{P} \quad (2)$$

The quantum efficiency (η), that measures the number of charge carriers collected per incident photon, has been calculated from responsivity by following formula:

$$\eta = R \frac{h\nu}{e} \quad (3)$$

where $h\nu$ is the photon energy and e the elementary charge.

Figure 6 shows the spectral responsivity curve, at 0 V bias, in the UV range, from 210 to 385 nm. In the same plot, the corresponding quantum efficiency characteristics are reported.

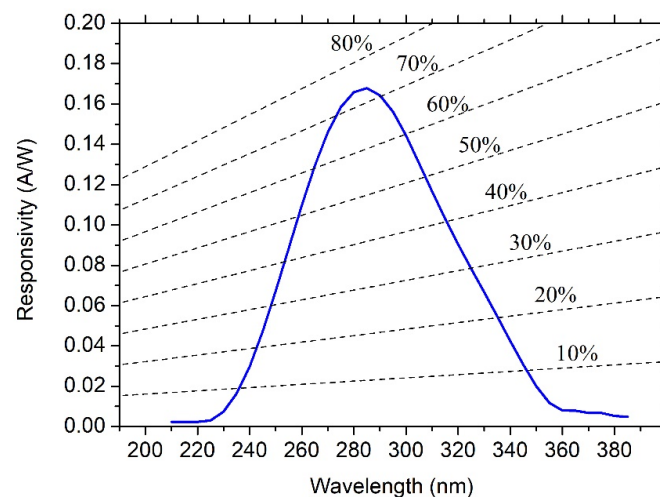


Figure 6. Responsivity and quantum efficiency (%) of the 4H-SiC photodiode as a function of wavelength.

To our knowledge, the calculated responsivity peak of 0.168 A/W, found at the wavelength of 285 nm, is the best value ever reported for UV photodiodes with no bias applied. A comparison between Schottky and p-i-n based UV photodiodes, reported in the literature to date, is shown in Table 1.

Table 1. Responsivity and Q.E. comparison for Schottky and p-i-n based UV photodiodes reported in the literature to date.

Ref.	Device	Responsivity Peak (A/W)	Reverse Voltage (V)	Wavelength at Peak (nm)	Q.E. (%)	Thermal Stability
[15]	Schottky	0.093	−15	270	42.5	n.a.
[16]	Schottky	0.115	0	285	50.0	200 °C
[20]	p-i-n	0.096	0	270	44.4	175 °C
[21]	p-i-n	0.13	0	266	n.a.	450 K
[22]	p-i-n	0.13	−5	270	61	180 °C
[This work]	p-i-n	0.168	0	285	72.7	350 °C
		0.204	−30		88.3	

Figure 7 shows the responsivity peak and quantum efficiency as functions of the reverse bias voltage at $\lambda = 285$ nm. It is shown that higher responsivity and quantum efficiency are achieved as the reverse bias increases. This fact is attributed to the expansion of the depletion region that enhances the collection efficiency and, therefore, the separation

mechanism of the photogenerated carriers [29], which, in turn, boosts the device’s current capability.

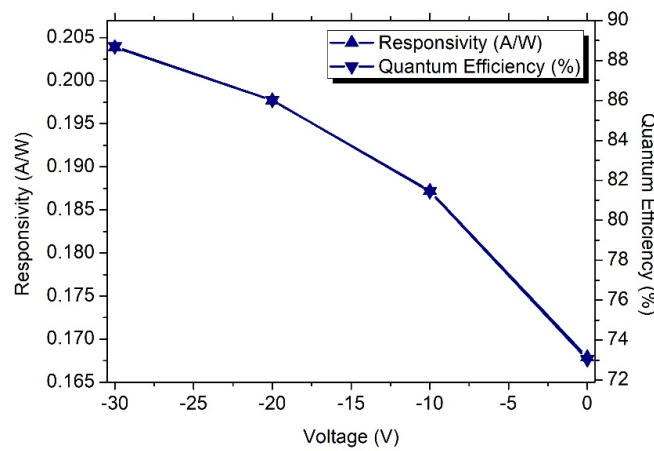


Figure 7. Responsivity peak and corresponding quantum efficiency as functions of the reverse bias voltage.

The peak values of both responsivity and quantum efficiency for different biasing voltages are summarized in Table 2.

Table 2. Responsivity and quantum efficiency for different bias condition at a 285-nanometer wavelength.

Reverse Bias	Responsivity Peak (A/W)	Quantum Efficiency (%)
0 V	0.168	72.7
10 V	0.187	81.1
20 V	0.198	85.6
30 V	0.204	88.3

Finally, the 4H-SiC photodiode has been characterized in terms of viewing angles in a dark room at RT. The photodiode, placed always at the same distance of 7 cm from the monochromator output, was subjected to an UV radiation at the wavelength of $\lambda = 285$ nm. The following measurements, shown in Figure 8, were performed with viewing angles between -45° and $+45^\circ$, in steps of 5° .

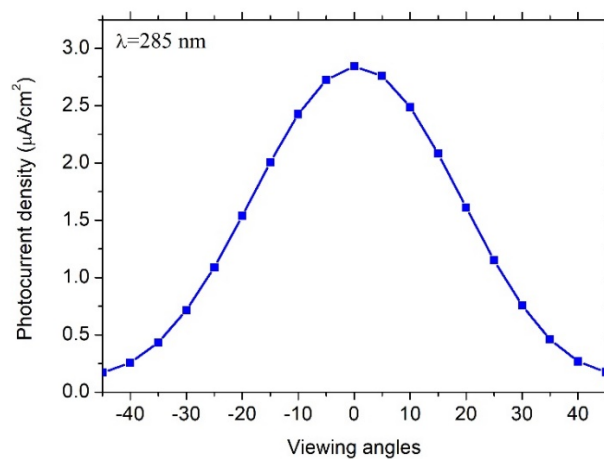


Figure 8. 4H-SiC photodiode photocurrent density at varying viewing angles.

4. Analysis of High-Temperature Effects

A full characterization of the 4H-SiC photodiode was performed taking into account the effects on the device performances after deep cycles of thermal stress. These measurements were carried out in an adiabatic chamber, where temperatures up to 350 °C are reached.

In particular, ten cycles of measurements were iterated, in a long period of time, from RT up to 350 °C and vice versa, in order to verify the photodiode optical and electrical stability at the end of such thermal stress. Moreover, the same device under test (DUT) has been kept at 350 °C for 24 h, and afterwards, the IV characteristics in dark condition and under UV illumination were measured at RT.

Figure 9 shows the responsivity curves as measured pre- and post the provided thermal sollicitation, leading to a very good reproducibility of the spectral photodiode output response.

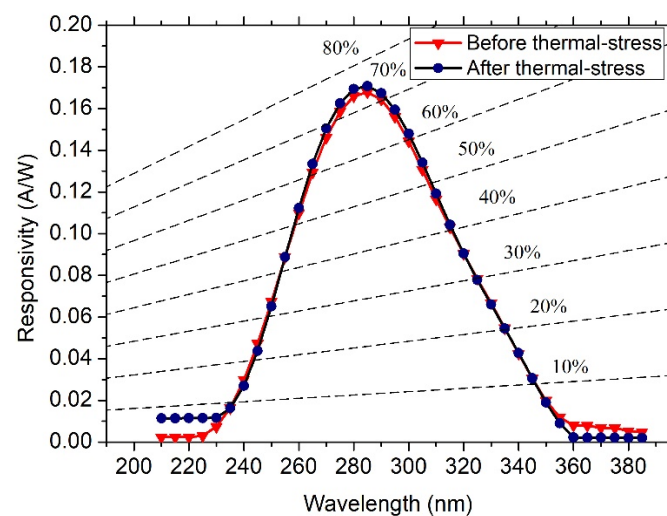


Figure 9. 4H-SiC p-i-n photodiode responsivities before and after ten cycles of measurements, from RT up to 350 °C and vice versa. During the last cycle, the DUT has been kept at $T = 350$ °C for 24 h.

5. Conclusions

In this paper, we focused on an investigation of the electro-optical performances related to a 4H-SiC p-i-n photodiode fabricated via an ion implantation technique. At -10 V, a low value of the dark reverse current density is detected, $J_D = 38.6$ nA/cm², allowing the photocurrent to be correctly measured under UV radiation. At the wavelength of $\lambda = 285$ nm, the photo-response peak is 0.204 A/W at -30 V, providing a better value if compared to those found in the literature, including Schottky photodiode, p-i-n, and more sophisticated bipolar devices. Moreover, the calculated quantum efficiency is 72.7%, the best value ever reported for UV photodiodes with no bias applied.

Furthermore, the photodiode performance has been analyzed after several cycles of thermal stress with temperatures up to 350 °C showing a stable optical response, even after different long time thermal sollicitations. This last feature is welcomed by research community and industry, above all when 4H-SiC-based UV detectors must operate in critical applications where the sensitivity to thermal stress is a critical issue.

Author Contributions: Conceptualization, S.R. and F.G.D.C.; Data curation, S.R., E.D.M. and F.G.D.C.; Formal analysis, S.R., M.L.M., H.B., L.D. and F.G.D.C.; Investigation, S.R.; Methodology, S.R.; Supervision, S.R. and F.G.D.C.; Validation, S.R. and F.G.D.C.; Writing—original draft, S.R.; Writing—review & editing, S.R., L.D., E.D.M., F.P. and F.G.D.C. All authors have read and agreed to the published version of the manuscript.

Funding: This research received no external funding.

Data Availability Statement: Data is contained within the article.

Acknowledgments: Roberta Nipoti and the Clean Room staff of the CNR-IMM Unit of Bologna (Italy) are thankfully recognized for providing the p-i-n diode and for stimulating discussions.

Conflicts of Interest: The authors declare no conflict of interest.

References

1. Chen, X.; Ren, F.; Gu, S.; Ye, J. Review of gallium-oxide-based solar-blind ultraviolet photodetectors. *Photonics Res.* **2019**, *7*, 381–415. [CrossRef]
2. Araujo, H.M.; Chepel, V.Y.; Lopes, M.I.; Marques, R.F.; Policarpo, A.J.P.L. Low temperature performance of photomultiplier tubes illuminated in pulsed mode by visible and vacuum ultraviolet light. *Rev. Sci. Instrum.* **1997**, *68*, 34–40. [CrossRef]
3. De Arquer, F.P.G.; Armin, A.; Meredith, P.; Sargent, E.H. Solution-processed semiconductors for next-generation photodetectors. *Nat. Rev. Mater.* **2017**, *2*, 16100. [CrossRef]
4. Zhou, D.; Liu, F.; Lu, H.; Chen, D.; Ren, F.; Zhang, R.; Zheng, Y. High-temperature single photon detection performance of 4H-SiC avalanche photodiodes. *IEEE Photonics Technol. Lett.* **2014**, *26*, 1136–1138. [CrossRef]
5. Sozzi, G.; Puzanghera, M.; Menozzi, R.; Nipoti, R. The role of defects on forward current in 4H-SiC pin diodes. *IEEE Trans. Electron Devices* **2019**, *66*, 3028–3033. [CrossRef]
6. Hou, S.; Hellström, P.; Zetterling, C.; Östling, M. 550 °C 4H-SiC p-i-n Photodiode Array with Two-Layer Metallization. *IEEE Electron Device Lett.* **2016**, *37*, 1594–1596. [CrossRef]
7. Hou, S.; Hellström, P.; Zetterling, C.; Östling, M. Scaling of 4H-SiC p-i-n photodiodes for high temperature applications. In Proceedings of the 2017 75th Annual Device Research Conference (DRC), South Bend, IN, USA, 25–28 June 2017; pp. 1–2.
8. Sang, L.; Liao, M.; Sumiya, M. A comprehensive review of semiconductor ultraviolet photodetectors: From thin film to one-dimensional nanostructures. *Sensors* **2013**, *13*, 10482–10518. [CrossRef]
9. Bencherif, H.; Dehimi, L.; Messina, G.; Vincent, P.; Pezzimenti, F.; Della Corte, F.G. An optimized Graphene/4H-SiC/Graphene MSM UV-photodetector operating in a wide range of temperature. *Sens. Actuators A Phys.* **2020**, *307*, 112007. [CrossRef]
10. Seely, J.F.; Kjornrattanawanich, B.; Holland, G.E.; Korde, R. Response of a SiC photodiode to extreme ultraviolet through visible radiation. *Opt. Lett.* **2005**, *30*, 3120–3122. [CrossRef]
11. Rao, S.; Pangallo, G.; Della Corte, F.G. 4H-SiC p-i-n diode as Highly Linear Temperature Sensor. *IEEE Trans. Electron Devices* **2016**, *63*, 414–418. [CrossRef]
12. Rao, S.; Pangallo, G.; Della Corte, F.G. Highly Linear Temperature Sensor Based on 4H-Silicon Carbide p-i-n diodes. *IEEE Electron Device Lett.* **2015**, *36*, 1205–1208. [CrossRef]
13. Rao, S.; Pangallo, G.; Pezzimenti, F.; Della Corte, F.G. High-performance temperature sensor based on 4H-SiC Schottky diodes. *IEEE Electron Device Lett.* **2015**, *36*, 720–722. [CrossRef]
14. Zeghdar, K.; Dehimi, L.; Pezzimenti, F.; Rao, S.; Della Corte, F.G. Simulation and analysis of the current–voltage–temperature characteristics of Al/Ti/4H-SiC Schottky barrier diodes. *Jpn. J. Appl. Phys.* **2019**, *58*, 014002. [CrossRef]
15. Lioliou, G.; Mazzillo, M.C.; Sciuto, A.; Barnett, A.M. Electrical and ultraviolet characterization of 4H-SiC Schottky photodiodes. *Opt. Express* **2015**, *23*, 21657–21670. [CrossRef] [PubMed]
16. Xu, Y.; Zhou, D.; Lu, H.; Chen, D.; Ren, F.; Zhang, R.; Zheng, Y. High-temperature and reliability performance of 4H-SiC Schottky-barrier photodiodes for UV detection. *J. Vac. Sci. Technol. B Nanotechnol. Microelectron. Mater. Process. Meas. Phenom.* **2015**, *33*, 040602. [CrossRef]
17. Li, L.; Zhou, D.; Liu, F.; Lu, H.; Ren, F.; Chen, D.; Zhang, R.; Zheng, Y. High fill-factor 4H-SiC avalanche photodiodes with partial trench isolation. *IEEE Photonics Technol. Lett.* **2016**, *28*, 2526–2528. [CrossRef]
18. Ng, B.K.; Yan, F.; David, J.P.R.; Tozer, R.C.; Rees, G.J.; Qin, C.; Zhao, J.H. Multiplication and excess noise characteristics of thin 4H-SiC UV avalanche photodiodes. *IEEE Photonics Technol. Lett.* **2002**, *14*, 1342–1344. [CrossRef]
19. Zhou, Q.; Liu, H.D.; McIntosh, D.C.; Hu, C.; Zheng, X.; Campbell, J.C. Proton-implantation-isolated 4H-SiC avalanche photodiodes. *IEEE Photonics Technol. Lett.* **2009**, *21*, 1734–1736. [CrossRef]
20. Yang, S.; Zhou, D.; Lu, H.; Chen, D.; Ren, F.; Zhang, R.; Zheng, Y. High-performance 4H-SiC pin ultraviolet photodiode with p layer formed by Al implantation. *IEEE Photonics Technol. Lett.* **2016**, *28*, 1189–1192. [CrossRef]
21. Cai, J.; Chen, X.; Hong, R.; Yang, W.; Wu, Z. High-performance 4H-SiC-based pin ultraviolet photodiode and investigation of its capacitance characteristics. *Opt. Commun.* **2014**, *333*, 182–186. [CrossRef]
22. Chen, X.; Zhu, H.; Cai, J.; Wu, Z. High-performance 4H-SiC-based ultraviolet p-i-n photodetector. *J. Appl. Phys.* **2007**, *102*, 024505. [CrossRef]
23. CNR-Institute for Microelectronics and Microsystem (IMM) of Bologna. Available online: <https://www.cnr.it/en/institute/057/institute-for-microelectronics-and-microsystems-imm> (accessed on 13 October 2021).
24. Keeping Pace with the World’s Demand for SiC Power. Available online: <https://www.wolfspeed.com/products/materials/n-type-sic-substrates> (accessed on 13 October 2021).
25. Nipoti, R.; Puzanghera, M.; Sozzi, G.; Menozzi, R. Perimeter and Area Components in the I–V Curves of 4H-SiC Vertical p+-in Diode with Al+ Ion-Implanted Emitters. *IEEE Trans. Electron Devices* **2017**, *65*, 629–635. [CrossRef]

-
26. Poggi, A.; Bergamini, F.; Nipoti, R.; Solmi, S.; Canino, M.; Carnera, A. Effects of heating ramp rates on the characteristics of Al implanted 4H-SiC junctions. *Appl. Phys. Lett.* **2006**, *88*, 162106. [[CrossRef](#)]
 27. Wan, X.; Xu, Y.; Guo, H.; Shehzad, K.; Ali, A.; Liu, Y.; Yang, J.; Dai, D.; Lin, C.T.; Liu, L.; et al. A self-powered high-performance graphene/silicon ultraviolet photodetector with ultra-shallow junction: Breaking the limit of silicon? *NPJ 2D Mater. Appl.* **2017**, *1*, 4. [[CrossRef](#)]
 28. DET210/M. Available online: <https://www.thorlabs.com/thorproduct.cfm?partnumber=DET210/M> (accessed on 13 October 2021).
 29. Karanth, S.P.; Sumesh, M.A.; Shobha, V.; Sirisha, J.; Yadav, D.; Vijay, S.B.; Sriram, K.V. Electro-Optical Performance Study of 4H-SiC/Pd Schottky UV Photodetector Array for Space Applications. *IEEE Trans. Electron Devices* **2020**, *67*, 3242–3249. [[CrossRef](#)]